

Higgs Boson Resummation via Bottom-Quark Fusion

B. Field*

*C.N. Yang Institute for Theoretical Physics, Stony Brook University, Stony Brook, New York 11794-3840, USA and
Department of Physics, Brookhaven National Laboratory, Upton, New York 11973, USA*

(Dated: July 21, 2004)

The region of small transverse momentum in $q\bar{q}$ - and gg -initiated processes must be studied in the framework of resummation to account for the large, logarithmically-enhanced contributions to physical observables. In this letter, we study resummed differential cross-sections for Higgs production via bottom-quark fusion. We find that the differential distribution peaks at approximately 15 GeV, a number of great experimental importance to measuring this production channel.

PACS numbers: 13.85.-t, 14.80.Bn, 14.80.Cp

Resummation of total and differential cross-section for the inclusive production of a Higgs boson has concentrated on the gluon-gluon initial state[1, 2, 3, 4, 5, 6, 7, 8, 9, 10, 11, 12, 13, 14]. In the Standard Model (SM), the gluon-gluon initial state gives the largest contribution to the total and differential cross-sections, but this is not always the case in extensions of the SM. In the Minimal Supersymmetric Standard Model (MSSM) the bottom-quark fusion initial state can be greatly enhanced, perhaps leading to the observation of a supersymmetric signal in nature, if the location of the peak of the differential distribution is known.

The MSSM contains two Higgs doublets, one giving mass to up-type quarks and the other to down-type quarks. The associated vacuum expectation values (VEVs) are labeled v_u and v_d respectively, and fix the free MSSM parameter $\tan\beta \equiv v_u/v_d$. In the MSSM, there are five physical Higgs boson mass eigenstates. In this letter, we are interested in the neutral Higgs bosons $\{h^0, H^0, A^0\}$ which we will call Φ generically.

In contrast to the SM, the bottom-quark Yukawa couplings in the MSSM can be enhanced with respect to the top-quark Yukawa coupling. In the SM, the ratio of the $t\bar{t}\Phi$ and $b\bar{b}\Phi$ couplings is given at tree-level by $\lambda_t^{\text{SM}}/\lambda_b^{\text{SM}} = m_t/m_b \approx 35$. In the MSSM, the coupling depends on the value of $\tan\beta$. At leading order,

$$\frac{\lambda_t^{\text{MSSM}}}{\lambda_b^{\text{MSSM}}} = f_\Phi \frac{1}{\tan\beta} \cdot \frac{m_t}{m_b}, \quad (1)$$

with

$$f_\Phi = \begin{cases} -\cot\alpha, & \Phi = h^0 \\ \tan\alpha, & \Phi = H^0 \\ \cot\beta, & \Phi = A^0 \end{cases} \quad (2)$$

where α is the mixing angle between the weak and the mass eigenstates of the neutral scalars. Given the mass of the pseudoscalar M_{A^0} and $\tan\beta$, the angle α can be determined given reasonable assumptions for the masses of the other supersymmetric particles in the spectrum.

The form of f_Φ shows us that the production of the pseudoscalar due to bottom-quark fusion is enhanced by a factor of $\tan^2\beta$, which is a free parameter in the theory.

THE BOTTOM-QUARK

It is also important to define what is meant by a bottom-quark distribution[15, 16, 17]. In our analysis, we employed the CTEQ6.1M bottom-quark parton distribution[18] with $\alpha_s(M_Z) = 0.118$ and set the mass of the Higgs boson of interest $M_\Phi = 120$ GeV. We compared the bottom-quark distribution function in the PDF set and the numeric solution to the Dokshitzer-Gribov-Lipatov-Altarelli-Parisi (DGLAP) equations for a single quark splitting. A bottom-quark distribution for a gluon splitting into a $b\bar{b}$ pair can be written in the DGLAP formalism as

$$\tilde{b}(x, \mu) = \frac{\alpha_s(\mu)}{2\pi} \ln\left(\frac{\mu^2}{m_b^2}\right) \int_x^1 \frac{dy}{y} P_{q \leftarrow g}\left(\frac{x}{y}\right) g(y, \mu), \quad (3)$$

where g is the gluon distribution, and the DGLAP splitting function is

$$P_{q \leftarrow g}(z) = \frac{1}{2}[z^2 + (1-z)^2]. \quad (4)$$

The bottom-quark distribution is encoded into the CTEQ PDF set in this manner[19], but takes into account multiple quark splitting functions. When evaluated with the DGLAP formalism, we found the differential cross-section increased by approximately 10% near its peak. However, we used the native bottom-quark distributions for speed and to understand their built-in uncertainties.

Previously[14], we calculated in detail the resummation coefficients for a differential cross-section for the scalar and pseudoscalar Higgs boson from the gluon-gluon initial state. In this letter, we will calculate the resummation coefficients needed for the resummation of the $b\bar{b}$ initial state for the scalar and pseudoscalar Higgs bosons in the same manner as the gluon-gluon channel in Ref. [14]. We will leave the bottom-quark-Higgs coupling set equal to the SM value so that the reader can scale the results to whatever coupling value is of interest.

RESUMMATION

The resummation formalism needs the lowest order total cross-section as a normalization factor (see [14] for details), $b\bar{b} \rightarrow \Phi$ in this case. Following Ref. [20], we will ignore the bottom-quark mass except in the Yukawa coupling with the Higgs boson. Although the pseudoscalar Higgs couples to quarks with a γ_5 , there are no differences in the matrix elements (modulo the MSSM coupling factor) when the bottom-quark mass is neglected.

It is important to use the $\overline{\text{MS}}$ running mass for the bottom-quark in our calculation as the difference from the pole mass at the scales involved is considerable[21, 22]. In the SM, the bottom-quark Yukawa coupling is $\lambda_b^{\text{SM}} = \sqrt{2}\overline{m}_b/v$, where v is the SM VEV and is approximately equal to 246 GeV and \overline{m}_b is the $\overline{\text{MS}}$ running mass. We have set the bottom-quark mass $\overline{m}_b(\overline{m}_b) = 4.62$ GeV in our calculations. The NLO running of the bottom-quark mass corresponds to $\overline{m}_b(M_\Phi) = 3.23$ GeV. The coupling in the MSSM can be written

$$\lambda_b^{\text{MSSM}} = \begin{cases} -\sqrt{2} \frac{\overline{m}_b}{v} \frac{\sin \alpha}{\cos \beta}, & \Phi = h^0 \\ \sqrt{2} \frac{\overline{m}_b}{v} \frac{\cos \alpha}{\cos \beta}, & \Phi = H^0 \\ \sqrt{2} \frac{\overline{m}_b}{v} \tan \beta, & \Phi = A^0. \end{cases} \quad (5)$$

The spin- and color-averaged total partonic cross-section (see Fig. 1a) for the leading order subprocess, $b\bar{b} \rightarrow \Phi$, can be easily written

$$\hat{\sigma}_0^{\text{SM}} = \frac{6\pi}{4N_c^2} \frac{\overline{m}_b^2}{v^2} \frac{1}{M_\Phi^2} \delta(1-z), \quad (6)$$

where $z = M_\Phi^2/\hat{s}$ and the number of colors $N_c = 3$. We also need the LO differential cross-section (Fig. 1c) for the next-to-leading log (NLL) resummation coefficients for the differential cross-section. If we remove the $\delta(1-z)$ factor from our prefactor $\hat{\sigma}_0$, then we can write the spin- and color-averaged differential cross-section for $b(p_1)\bar{b}(p_2) \rightarrow g(-p_3)\Phi(-p_5)$ as

$$\begin{aligned} \frac{d\hat{\sigma}}{d\hat{t}} &= \hat{\sigma}_0 \left(\frac{\alpha_s}{\pi} \right) \frac{C_F}{2} \left(\frac{M_\Phi^4 + \hat{s}^2}{\hat{s}\hat{t}\hat{u}} \right) \\ &= \hat{\sigma}_0 \left(\frac{\alpha_s}{\pi} \right) \frac{C_F}{2} \frac{1}{p_t^2} \left[1 + z^2 \right]. \end{aligned} \quad (7)$$

where $C_F = (N_c^2 - 1)/2N_c$, and the kinematic variables are defined as $\hat{s} = (p_1 + p_2)^2$, $\hat{t} = (p_1 + p_5)^2$, $\hat{u} = (p_2 + p_5)^2$, and $M_\Phi^2 = p_5^2$. In our second line, we have written the differential cross-section in terms of $\hat{u}\hat{t} = p_t^2\hat{s}$ for the $2 \rightarrow 2$ process.

To find the resummation coefficients for a differential cross-sections[2, 4, 9, 14] we integrate the differential cross-section around $p_t = 0$

$$\Delta\hat{\sigma} = \int_0^{q_t^2} dp_t^2 \frac{d\hat{\sigma}}{dp_t^2} \quad (8)$$

and label this result ‘real’ as it is similar to the real corrections to the LO total cross-section. Working in $N = 4 - 2\epsilon$ dimensions, we find

$$\begin{aligned} \Delta\hat{\sigma}^{\text{real}} &= \hat{\sigma}_0 z \frac{\alpha_s}{\pi} \left[\frac{C_F}{\epsilon^2} + \frac{3}{2} \frac{C_F}{\epsilon} - \frac{C_F}{2} \ln^2 \left(\frac{M_\Phi^2}{q_t^2} \right) \right. \\ &\quad \left. + \frac{3}{2} C_F \ln \left(\frac{M_\Phi^2}{q_t^2} \right) + C_F - C_F \zeta_2 \right]. \end{aligned} \quad (9)$$

To regularize this result, we need to add the virtual corrections that are shown in Fig. 1b. These corrections are very similar to Drell-Yan corrections[23]. The virtual corrections can be written as

$$\Delta\hat{\sigma}^{\text{virt}} = \hat{\sigma}_0 \left(\frac{\alpha_s}{\pi} \right) \left[-\frac{C_F}{\epsilon^2} - \frac{3}{2} \frac{C_F}{\epsilon} - C_F + 2C_F \zeta_2 \right]. \quad (10)$$

In the Drell-Yan case, the $-C_F$ factor would be $-4C_F$. When the two results are added together the resummation coefficients are easily read off from the expression. The total expression is

$$\begin{aligned} \Delta\hat{\sigma} &= \hat{\sigma}_0 z \left[1 + \frac{\alpha_s}{\pi} \left(-\frac{C_F}{2} \ln^2 \left(\frac{M_\Phi^2}{q_t^2} \right) \right. \right. \\ &\quad \left. \left. + \frac{3}{2} C_F \ln \left(\frac{M_\Phi^2}{q_t^2} \right) + C_F \zeta_2 \right) \right]. \end{aligned} \quad (11)$$

Keeping with the notation of Ref. [14], we write these coefficients with an overbar as follows

$$\bar{A}_b^{(1)} = C_F, \quad \bar{B}_b^{(1)} = -\frac{3}{2} C_F, \quad \bar{C}_{b\bar{b}}^{(1)} = \frac{1}{2} C_F \zeta_2. \quad (12)$$

It is important to note that in contrast to W^\pm/Z^0 production and Drell-Yan processes[23, 24], the $\bar{C}^{(1)}$ coefficient is positive.

Finally, let us turn to determining the $C^{(1)}$ and $C^{(2)}$ coefficients for the total cross-section resummation, although total cross-sections will not be presented in this letter. Using the results of Ref. [20], we take the Mellin moments of the corrections in the limit $N \rightarrow \infty$ ($z \rightarrow 1$ in z -space). The NLO corrections are easy to color decompose due to the presence of only one color factor[14]. Leaving the terms that were originally proportional to the $\delta(1-z)$ factor inside curly brackets, we find

$$\Delta_{b\bar{b}}^{(1)} = \left[2C_F \right] \ln^2(N) + \left[2C_F \ln \frac{M_\Phi^2}{\mu_f^2} \right] \ln(N) + \left\{ 2C_F \zeta_2 - C_F + 2 \ln \frac{\mu_r^2}{\mu_f^2} \right\} + 2C_F \zeta_2 \quad (13)$$

where we have given both the renormalization scale μ_r and the factorization scale μ_f dependence in the results.

In contrast to NLO, the NNLO corrections contain a mix of color factors (both C_A and C_F appear). Although it is easy to see that the factor proportional to $\ln^4(N)$ should clearly be $2C_F^2$, no unique color decomposition from the results provided in Ref. [20] can be determined for all the terms in the expression. However, the numeric result can be written

$$\begin{aligned} \Delta_{b\bar{b}}^{(2)} = & \left[\frac{32}{9} \right] \ln^4(N) + \left[\frac{44}{9} - \frac{8}{27} n_f + \frac{64}{9} \ln \frac{M_\Phi^2}{\mu_f^2} \right] \ln^3(N) \\ & + \left[\frac{34}{3} + \frac{92}{9} \zeta_2 - \frac{20}{27} n_f + \left(\frac{38}{3} - \frac{4}{9} n_f \right) \ln \frac{M_\Phi^2}{\mu_f^2} \right. \\ & - \frac{16}{3} \ln \frac{M_\Phi^2}{\mu_f^2} + \frac{32}{9} \ln^2 \frac{M_\Phi^2}{\mu_f^2} \left. \right] \ln^2(N) + \left[\frac{404}{27} - 14 \zeta_3 \right. \\ & - \frac{56}{81} n_f + \left(\frac{34}{3} + \frac{92}{9} \zeta_2 - \frac{20}{27} n_f \right) \ln \frac{M_\Phi^2}{\mu_f^2} - \left(9 - \frac{2}{9} n_f \right) \\ & \times \ln^2 \frac{M_\Phi^2}{\mu_f^2} + \left(\frac{38}{3} - \frac{4}{9} n_f \right) \ln \frac{M_\Phi^2}{\mu_f^2} \ln \frac{M_\Phi^2}{\mu_r^2} \left. \right] \ln(N) + \left\{ \frac{115}{18} \right. \\ & + \frac{58}{9} \zeta_2 - \frac{26}{3} \zeta_3 - \frac{19}{18} \zeta_4 + \left(\frac{2}{27} - \frac{10}{27} \zeta_2 + \frac{2}{3} \zeta_3 \right) n_f \\ & + \left(\frac{25}{12} + \frac{38}{3} \zeta_2 \right) \ln \frac{M_\Phi^2}{\mu_r^2} - \left(\frac{1}{18} + \frac{4}{9} \zeta_2 \right) n_f \ln \frac{M_\Phi^2}{\mu_r^2} \\ & + \left(\frac{11}{12} - 10 \zeta_2 - \frac{122}{9} \zeta_3 \right) \ln \frac{M_\Phi^2}{\mu_f^2} + \left(\frac{1}{18} + \frac{4}{9} \zeta_2 \right) n_f \ln \frac{M_\Phi^2}{\mu_f^2} \\ & + \left(\frac{19}{4} - \frac{1}{6} n_f \right) \ln^2 \frac{M_\Phi^2}{\mu_r^2} + \left(\frac{19}{4} - \frac{32}{9} \zeta_2 - \frac{1}{6} n_f \right) \ln^2 \frac{M_\Phi^2}{\mu_f^2} \\ & + \left(\frac{1}{3} n_f - \frac{19}{2} \right) \ln \frac{M_\Phi^2}{\mu_r^2} \ln \frac{M_\Phi^2}{\mu_f^2} \left. \right\} + \frac{34}{3} \zeta_2 + \frac{88}{9} \zeta_3 + \frac{364}{45} \zeta_2 \\ & - \left(\frac{20}{27} \zeta_2 + \frac{16}{27} \zeta_3 \right) n_f + \left(\frac{38}{3} \zeta_2 - \frac{4}{9} \zeta_2 n_f \right) \ln \frac{M_\Phi^2}{\mu_r^2} \\ & - \left(\frac{16}{3} \zeta_2 - \frac{128}{9} \zeta_3 \right) \ln \frac{M_\Phi^2}{\mu_f^2} + \frac{32}{9} \zeta_2 \ln^2 \frac{M_\Phi^2}{\mu_f^2} \quad (14) \end{aligned}$$

We can also determine the NNLL $A^{(2)}$ and $B^{(2)}$ coefficients. $A^{(2)}$ agrees with a previous calculation[25]. We find

$$A_b^{(1)} = C_F \quad (15)$$

$$A_b^{(2)} = \frac{1}{2} C_F \left(C_A \left(\frac{67}{18} - \zeta_2 \right) - \frac{10}{9} n_f T_R \right) \quad (16)$$

for $A^{(1)}$ and $A^{(2)}$ and

$$B_b^{(1)} = -\frac{3}{2} C_F \quad (17)$$

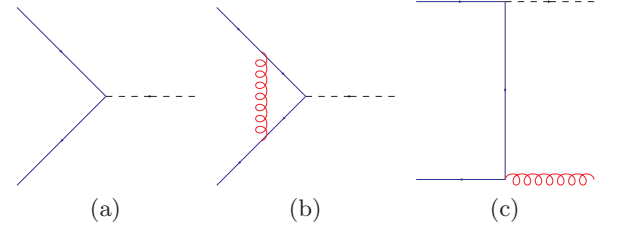


FIG. 1: Diagrams needed for the $b\bar{b}$ initial state resummed differential cross-section. Figure 1a is the lowest order production channel and couples differently for different Higgs bosons. Figure 1b is the virtual correction to the lowest order process. Figure 1c is the lowest order graph contributing to the differential cross-section. The crossed graph is not shown.

$$\begin{aligned} B_b^{(2)} = & C_F^2 \left(\frac{3}{2} \zeta_2 - 3 \zeta_3 - \frac{3}{16} \right) \\ & - C_A C_F \left(\frac{11}{18} \zeta_2 - \frac{3}{2} \zeta_3 + \frac{13}{16} \right) \\ & - n_f C_F T_R \left(\frac{1}{4} + \frac{2}{9} \zeta_2 \right) \quad (18) \end{aligned}$$

for the $B^{(1)}$ and $B^{(2)}$ coefficients. The Mellin moments $\Delta_{b\bar{b}}^{(1)}$ and $\Delta_{b\bar{b}}^{(2)}$ are novel, as is $B_b^{(2)}$.

RESULTS AND CONCLUSIONS

The differential resummation coefficients and the position of the peak of the differential cross-section is of great interest to the experimental community involved with Higgs research at the LHC, particularly in the $M_\Phi = 120$ GeV mass range. Here the Higgs will decay primarily into $b\bar{b}$ pairs that can be tagged. Knowing where the peak of the differential distribution lies, especially if it is below the p_t of a typical trigger event, is of utmost importance. This letter will help in the analysis of the $b\bar{b}$ initial state.

The results of our calculations can be found in Figure 2. We have done our analysis for the LHC (a proton-proton collider at $\sqrt{S} = 14$ TeV). We find that the differential distribution at the LHC peaks at a transverse momentum of approximately 15 GeV. We find that the magnitude of the differential cross-section is an excellent match with previously published results[21, 22, 25]. The results for the Tevatron are extremely similar, but are smaller by a factor of 60 and the peak moves to a transverse momentum of approximately 13 GeV in the differential distribution.

A detailed study of the uncertainties in the calculation show that the uncertainty due to the PDF set is approximately 8 – 12%. At the peak of the distribution, the uncertainty is approximately 10% due to the PDFs. When

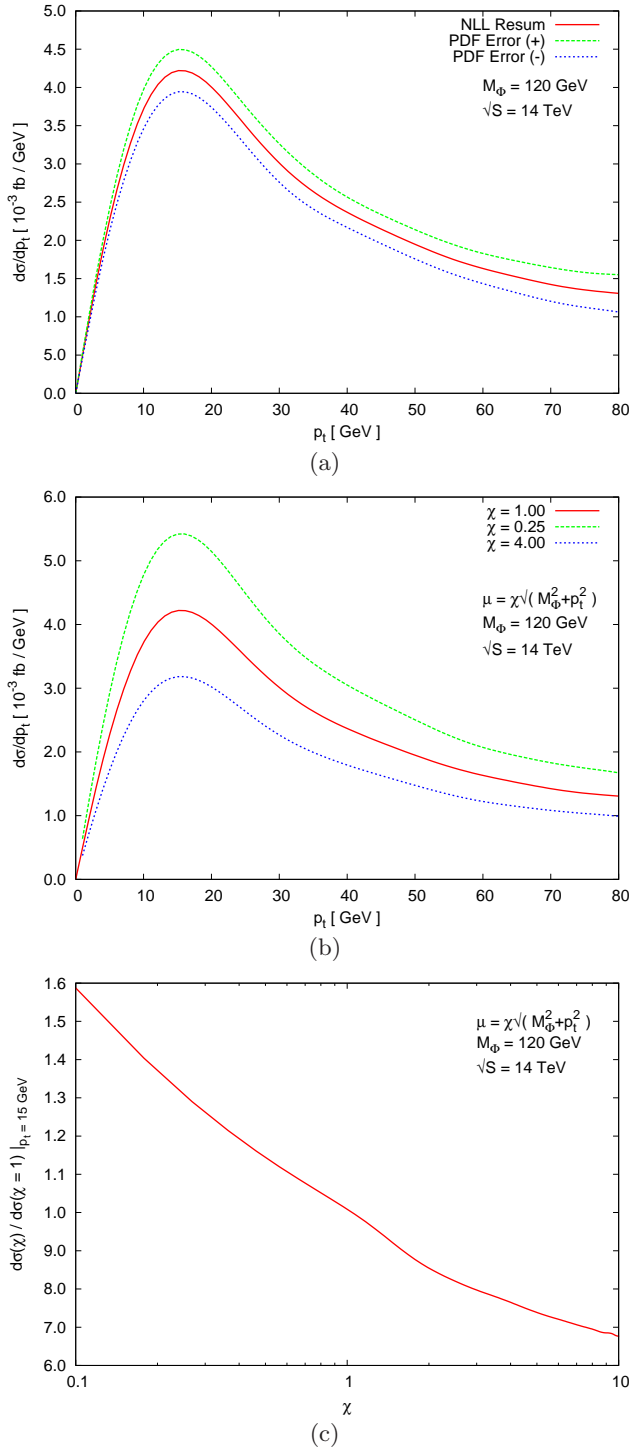


FIG. 2: Figure 2a shows the errors associated with the CTEQ6.1M PDF set. The variation is approximately 8–12%. Figure 2b show the variation of the renormalization and factorization scale for a factor of 1/4 and 4. These scales were chosen because there has been great interest in the scale $\mu = M_\Phi/4$. We find this variation to be approximately 20%. Figure 2c shows the movement of the peak of the differential distribution (at 15 GeV) for a variation in the scale by a factor of 10.

the scale is varied by a factor of four, we see a variation in the differential cross-section of approximately 20%. This would give us a combined uncertainty of 32%, which is slightly better than the gluon-gluon channel[14] uncertainty in the differential distribution. However, when the scale is only varied by a factor of two (as was the case for the gluon-gluon channel), the total uncertainty drops to 25%.

We have calculated the resummation coefficients needed for NLL inclusive Higgs production via bottom-quark fusion in the SM and the MSSM for the differential cross-section and for the NNLL resummation for the total cross-section. We find a smaller uncertainty in the bottom-quark initial state than the gluon-gluon initial state.

The author would like to acknowledge the help and comments of J. Smith, S. Dawson, G. Sterman, W. Vogelsong, F. Olness, and A. Field-Pollatou. I would also like to thank W. Kilgore and R. Harlander for supplying the output of their calculation[20] including its scale dependence.

* bfield@ic.sunysb.edu

- [1] S. Catani and L. Trentadue, Nucl. Phys. B **327**, 323 (1989).
- [2] R. P. Kauffman, Phys. Rev. D **44**, 1415 (1991).
- [3] C. P. Yuan, Phys. Lett. B **283**, 395 (1992).
- [4] R. P. Kauffman, Phys. Rev. D **45**, 1512 (1992).
- [5] S. Catani, M. L. Mangano, P. Nason and L. Trentadue, Nucl. Phys. B **478**, 273 (1996) [arXiv:hep-ph/9604351].
- [6] M. Kramer, E. Laenen and M. Spira, Nucl. Phys. B **511**, 523 (1998).
- [7] C. Balazs and C. P. Yuan, Phys. Lett. B **478**, 192 (2000) [arXiv:hep-ph/0001103].
- [8] D. de Florian and M. Grazzini, Phys. Rev. Lett. **85**, 4678 (2000) [arXiv:hep-ph/0008152].
- [9] D. de Florian and M. Grazzini, Nucl. Phys. B **616**, 247 (2001) [arXiv:hep-ph/0108273].
- [10] C. J. Glosser and C. R. Schmidt, JHEP **0212**, 016 (2002) [arXiv:hep-ph/0209248].
- [11] E. L. Berger and J.-w. Qiu, Phys. Rev. D **67**, 034026 (2003) [arXiv:hep-ph/0210135].
- [12] E. L. Berger and J.-w. Qiu, Phys. Rev. Lett. **91**, 222003 (2003) [arXiv:hep-ph/0304267].
- [13] G. Bozzi, S. Catani, D. de Florian and M. Grazzini, Phys. Lett. B **564**, 65 (2003) [arXiv:hep-ph/0302104].
- [14] B. Field, In Press, Phys. Rev. D, [arXiv:hep-ph/0405219].
- [15] F. I. Olness and W. K. Tung, Nucl. Phys. B **308**, 813 (1988).
- [16] R. M. Barnett, H. E. Haber and D. E. Soper, Nucl. Phys. B **306**, 697 (1988).
- [17] F. I. Olness, R. J. Scalise and W. K. Tung, Phys. Rev. D **59**, 014506 (1999) [arXiv:hep-ph/9712494].
- [18] J. Pumplin, D. R. Stump, J. Huston, H. L. Lai, P. Nadolsky and W. K. Tung, JHEP **0207**, 012 (2002) [arXiv:hep-ph/0201195].
- [19] F. I. Olness, private communication.

- [20] R. V. Harlander and W. B. Kilgore, Phys. Rev. D **68**, 013001 (2003) [arXiv:hep-ph/0304035].
- [21] J. Campbell, R. K. Ellis, F. Maltoni and S. Willenbrock, Phys. Rev. D **67**, 095002 (2003) [arXiv:hep-ph/0204093].
- [22] D. Dicus, T. Stelzer, Z. Sullivan and S. Willenbrock, Phys. Rev. D **59**, 094016 (1999) [arXiv:hep-ph/9811492].
- [23] G. Altarelli, R. K. Ellis and G. Martinelli, Nucl. Phys. B **157**, 461 (1979).
- [24] P. B. Arnold and R. P. Kauffman, Nucl. Phys. B **349**, 381 (1991).
- [25] C. Balazs, H. J. He and C. P. Yuan, Phys. Rev. D **60**, 114001 (1999) [arXiv:hep-ph/9812263].